PHYSICAL REVIEW B **93**, 180301(R) (2016)

Quantum resonance catastrophe for conductance through a periodically driven barrier

Daniel Thuberg,[1] Sebastián A. Reyes,[1] and Sebastian Eggert[2]
[1]*Instituto de Física, Pontificia Universidad Católica de Chile, Casilla 306, Santiago 22, Chile*
[2]*Physics Department and Research Center OPTIMAS, University of Kaiserslautern, D-67663 Kaiserslautern, Germany*
(Received 13 October 2015; revised manuscript received 29 February 2016; published 9 May 2016)

We consider the quantum conductance in a tight-binding chain with a locally applied potential which is oscillating in time. The steady state for such a driven impurity can be calculated exactly for any energy and applied potential using the Floquet formalism. The resulting transmission has a nontrivial, nonmonotonic behavior depending on incoming momentum, driving frequency, and the strength of the applied periodic potential. Hence there is an abundance of tuning possibilities, which allows finding the resonances of total reflection for any choice of incoming momentum and periodic potential. Remarkably, this implies that even for an arbitrarily small infinitesimal impurity potential it is always possible to find a resonance frequency at which there is a catastrophic breakdown of the transmission $T = 0$. The points of zero transmission are closely related to the phenomenon of Fano resonances at dynamically created bound states in the continuum. The results are relevant for a variety of one-dimensional systems where local AC driving is possible, such as quantum nanodot arrays, ultracold gases in optical lattices, photonic crystals, or molecular electronics.

DOI: 10.1103/PhysRevB.93.180301

Driven quantum systems appear in many different contexts in physics and chemistry [1–12]. At the same time there has been remarkable progress in the controlled design of tight-binding transport in nanoscale quantum systems with a high degree of coherence and tunability using molecular electronics [13–22], quantum dot arrays [3], or photonic materials [23–25]. Ultracold gases in optical lattices provide tight-binding models with a great variety of possible geometries [26], where dimensional crossover [27] and periodic driving [8–12] have been realized. For ultracold gases in optical lattices [26] it is now possible to insert localized impurities [28], which play the role of a local barrier that can easily be periodically changed using Feshbach resonances.

Theoretically there have been several studies on an alternating field along a wire [29,30], charge pumping [31], and a periodically driven Kondo impurity [32]. It is known that assisted and blocked tunneling is possible from periodic driving [3–8]. While the transport under general time-dependent potentials shows an abundance of physically interesting features [33] (including charge pumping), it appears that even for the most straightforward prototypical driven barrier there are unknown and remarkable conductance effects in the full frequency and amplitude dependence. In particular, we find that for a noninteracting tight-binding model with a periodically varying potential at one site, there is a complete breakdown of conductance even for an *infinitesimally small* amplitude, if the frequency ω is tuned to the corresponding resonance. We call this phenomenon the *quantum resonance catastrophe*, which is characterized by an extremely sharp linewidth and highly nonlinear switching and tuning opportunities. This is in contrast to the well-known phenomenon of tunneling, which allows nonzero transmission for any finite barrier.

The generic model system is described by a one-dimensional tight-binding chain for bosons or fermions with a periodically varying potential μ at one impurity site ($i = 0$)

$$H = -J \sum_i \left(c_i^\dagger c_{i+1} + c_{i+1}^\dagger c_i\right) - \mu \cos(\omega t) c_0^\dagger c_0, \qquad (1)$$

where we have used standard notation and the hopping amplitude is denoted by J. This model captures the essential physics of a single one-dimensional band, which is useful for the description of corresponding driven experimental setups mentioned above.

The goal of this paper is to calculate the transmission coefficient of an incoming particle with a given momentum k and corresponding energy $\epsilon = -2J\cos k$, which is the dispersion relation of the model in Eq. (1) away from the impurity. Just like in the static case, the transmission coefficient can be determined from the steady-state solution of the Schrödinger equation $(H(t) - i\partial_t)|\Psi(t)\rangle = 0$. Due to the periodicity of the Hamiltonian $H(t) = H(t + 2\pi/\omega)$ it is possible to use the Floquet formalism [2,34] to express any steady-state solution in terms of so-called Floquet states $|\Psi(t)\rangle = e^{-i\epsilon t}|\Phi(t)\rangle$, where ϵ is the quasienergy of the resulting $(d+1)$-dimensional eigenvalue equation $(H - i\partial_t)|\Phi(t)\rangle = \epsilon|\Phi(t)\rangle$ and the Floquet modes $|\Phi(t)\rangle = |\Phi(t + 2\pi/\omega)\rangle$ are periodic in time. Using the spectral decomposition

$$|\Phi(t)\rangle = \sum_{n=-\infty}^{\infty} e^{-in\omega t}|\Phi_n\rangle, \qquad (2)$$

the eigenvalue equation for a Hamiltonian of the form $H(t) = H_0 + 2H_1\cos(\omega t)$ becomes discrete in the time direction

$$H_0|\Phi_n\rangle + H_1(|\Phi_{n+1}\rangle + |\Phi_{n-1}\rangle) = (\epsilon + n\omega)|\Phi_n\rangle. \qquad (3)$$

A general steady state on the tight-binding lattice is given by

$$|\Phi_n\rangle = \sum_j \phi_{j,n} c_j^\dagger |0\rangle. \qquad (4)$$

The model in Eq. (1) therefore results in the following set of coupled equations:

$$-J(\phi_{-1,n} + \phi_{1,n}) - \frac{\mu}{2}(\phi_{0,n+1} + \phi_{0,n-1}) = (\epsilon + n\omega)\phi_{0,n},$$
$$-J(\phi_{j-1,n} + \phi_{j+1,n}) = (\epsilon + n\omega)\phi_{j,n} \quad \text{for} \quad j \neq 0, \qquad (5)$$

which effectively corresponds to a static Hamiltonian with eigenvalue ϵ for an infinite number of chains labeled by n, each

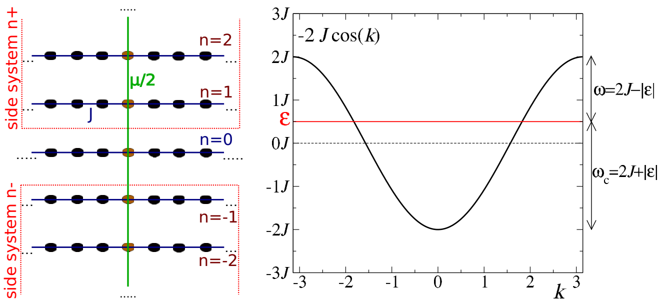

FIG. 1. Left: Sketch of the model mapped onto a set of static coupled chains. The $n = 0$ chain is locally connected to two side-coupled systems of chains with a corresponding chemical potential $n\omega$. Right: Dispersion relation with the special frequencies $\omega = 2J \pm \epsilon$ below which the side-coupled chains $n = \mp 1$ start to support unbound solutions for the case $\epsilon = 0.5J$.

with additional overall chemical potential of $n\omega$, analogous to a Wannier-Stark ladder [2]. The chains are coupled to each other only at site $j = 0$ by a hopping term $\mu/2$ as depicted in Fig. 1 (left). Notice that the entire problem is symmetric under parity transformation $j \to -j$, so that solutions are either parity symmetric or parity antisymmetric. The parity-antisymmetric solutions obey $\phi_{0,n} = 0$, $\forall n$, so they do not couple to the driving potential and can be ignored.

Transmission coefficient. We now want to calculate the transmission of an incoming particle with momentum k and $\epsilon = -2J\cos k$ for the chain $n = 0$. The parity symmetric solution is given by plane waves of the general form

$$\phi_{j,0} = A\cos(|j|k - \theta). \tag{6}$$

Since the potential μ only affects a single impurity site for all chains, the solutions for $j \neq 0$ must correspond to wavelike states (unbound solutions) for $|\epsilon + n\omega| < 2J$ and bound states otherwise according to Eq. (5). As indicated in Fig. 1 (right) a critical frequency can be defined:

$$\omega_c \equiv 2J + |\epsilon|. \tag{7}$$

For $\omega > \omega_c$ all chains with $n \neq 0$ are outside the band $|\epsilon + n\omega| > 2J$ and correspond to bound states. Below the frequency $\omega = \omega_c$ the first side-coupled chain starts to support unbound solutions. A second unbound solution starts to appear below $\omega = 2J - |\epsilon|$ and so on.

Let us first consider frequencies $\omega > \omega_c$ with bound states for all $n \neq 0$ of the form

$$\phi_{j,n} = C_n e^{-\kappa_n |j|}\,\mathrm{sign}(-n)^{j+n}, \tag{8}$$

where $\epsilon + n\omega = 2J\,\mathrm{sign}(n)\cosh\kappa_n$. Inserting these states into Eq. (5), we arrive at a recurrence relation for the coefficients C_n for $|n| > 0$,

$$\gamma_n C_n = C_{n-1} + C_{n+1} \text{ with } \gamma_n = \frac{2}{\mu}\sqrt{(\epsilon + n\omega)^2 - 4J^2}, \tag{9}$$

where we have defined $C_0 \equiv A\cos\theta$. The solution for this second-order recurrence relation is fixed up to an overall constant by requiring convergence for $|n| \to \infty$ and can be solved efficiently numerically. The angle θ is then given by

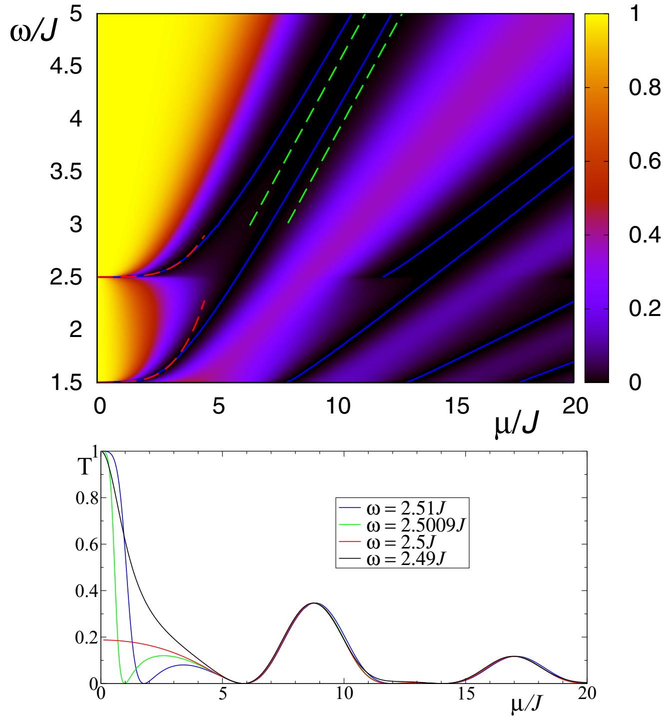

FIG. 2. Exact results for transmission coefficient T as a function of amplitude μ and frequency ω for an incoming wave of energy $\epsilon = 0.5J$. Top: The solid lines (blue) indicate the exact values of the resonances ($T = 0$) while the dashed lines are analytical expressions from the first zeros of Bessel functions $\mathcal{J}_{\pm\epsilon/\omega}$ in Eq. (13) at large frequencies and the small μ approximations in Eq. (14). Bottom: Behavior close to the critical frequency $\omega \approx \omega_c = 2.5J$. For $\omega = \omega_c$ the transmission approaches $T \to (2J - |\epsilon|)/8J$ as $\mu \to 0$.

Eq. (5) for $n = 0$ in terms of those coefficients

$$\tan\theta = \frac{\mu}{2u_k}\left(\frac{C_{-1}}{C_0} - \frac{C_1}{C_0}\right) \tag{10}$$

where we defined $u_k \equiv 2J\sin k$ as the particle velocity.

Since the bound states for $|n| > 0$ do not contribute in the transmission, it is now straightforward to calculate the transmission coefficient to be

$$T = \cos^2\theta = \frac{u_k^2}{u_k^2 + [\mu(C_{-1} - C_1)/2C_0]^2}. \tag{11}$$

The transmission obeys $T(\epsilon) = T(-\epsilon)$. For $\epsilon = 0$ the solution becomes symmetric $C_n = C_{-n}$, which results in $T(\epsilon = 0) = 1$ independent of μ for $\omega > \omega_c$ due to Klein tunneling [35]. In the following we assume $\epsilon \neq 0$.

Next we consider lower frequencies $\omega < \omega_c$, when unbound states also exist for $n \neq 0$. In this case it is useful to make an ansatz for an incoming wave at energy ϵ as well as transmitted and reflected waves in all unbound channels [36]. In this way it is possible to solve for all parameters. Finally, the total transmission coefficient can again be expressed by the solution of the recurrence relation in Eq. (9), which now involves the remaining bound states.

Results. Using this procedure the exact numerical solution for the transmission coefficient was obtained as shown in Fig. 2 for a given energy $\epsilon = 0.5J$ as a function of μ and ω. Perfect transmission $T \to 1$ can be observed for small μ or large frequencies. For increasing μ there is a sharp drop, however, and at special resonances a vanishing transmission $T = 0$ can be observed (blue solid lines). Interestingly, the transmission then increases again with increasing μ before more resonances with $T = 0$ are reached and so on. This apparent nonmonotonic behavior with potential μ and frequency ω can be understood in the high-frequency limit, where the recurrence relation can be solved analytically. In particular, note that $\gamma_n \to 2|n\omega + \epsilon|/\mu$ for $\omega \gg J$, so that Eq. (9) becomes exactly the defining recurrence relation for the Bessel functions [37] in this limit. For convergence as $|n| \to \infty$ the coefficients therefore can be chosen to be Bessel function of the first kind

$$C_n \approx \mathcal{J}_{|n+\epsilon/\omega|}(\mu/\omega). \tag{12}$$

The recurrence relation then approaches $C_0 \approx \mathcal{J}_{\pm\epsilon/\omega}$ for $n \to 0^\pm$ from above/below. Accordingly Eq. (10) can be approximated for $\omega \gg J$

$$\tan\theta \approx \frac{\mu}{2u_k}\left(\frac{\mathcal{J}_{1-\epsilon/\omega}(\mu/\omega)}{\mathcal{J}_{-\epsilon/\omega}(\mu/\omega)} - \frac{\mathcal{J}_{1+\epsilon/\omega}(\mu/\omega)}{\mathcal{J}_{\epsilon/\omega}(\mu/\omega)}\right). \tag{13}$$

These Bessel functions explain some of the observed features of T in Eq. (11), namely the oscillating behavior with μ and ω and resonances of $T = 0$ close to the zeros of the Bessel functions $\mathcal{J}_{\pm\epsilon/\omega}$, which are marked in Fig. 2 as dashed lines (green). Moreover, the behavior in Fig. 2 indeed only depends on the ratio μ/ω for large frequencies.

While the description in terms of Bessel functions is useful, this does not explain the behavior in the most interesting region close to $\omega \approx \omega_c$ where the data shows large gradients in the transmission coefficient. In Fig. 2 (bottom) the behavior changes dramatically with frequencies just above or below $\omega_c = 2.5J$ for small driving potential μ. There is a resonance with $T = 0$ which quickly shifts to smaller μ as the frequency is lowered ($\omega = 2.51J$ and $2.5009J$) and suddenly disappears completely once the $n = -1$ chain supports unbound solutions ($\omega = 2.49J$). Exactly at the critical frequency $\omega_c = 2.5J$ the results for $\mu \to 0$ show a well-behaved finite value $T \to (2J - |\epsilon|)/8J$, which corresponds to $C_{-1}^2/C_0^2 \to \gamma_{-2}^2$ and is neither close to unity nor zero. By looking very carefully one observes that there is another resonance close to $\mu \approx 11.5J$ which disappears at ω_c. Away from these singular points the changes of the transmission are very small, however, and appear to be continuous as the frequency goes through the critical value.

Resonances. It is worth noticing that the resonances $T = \cos^2\theta = 0$ for $\omega > \omega_c$ are special points at which the coefficient $\phi_{0,0} = C_0 = A\cos\theta$ vanishes exactly. In this case the side-coupled systems of the corresponding static problem in Eq. (5) become decoupled from the chain with $n = 0$ in Fig. 1 (left). Therefore, a resonance with $T = 0$ for $\omega > \omega_c$ occurs if and only if the isolated side system has an eigenenergy inside the band $|\epsilon| < 2J$.

This is a remarkable statement since the decoupled side chains for $n \neq 0$ only support bound states outside the band. However, due to the local coupling μ between the chains one of these energies is pushed inside the band, for which $T(\epsilon) = 0$. Such bound states in the continuum (BIC) were first proposed by von Neumann and Wigner for a *spatially* oscillating potential in the early days of quantum mechanics [38].

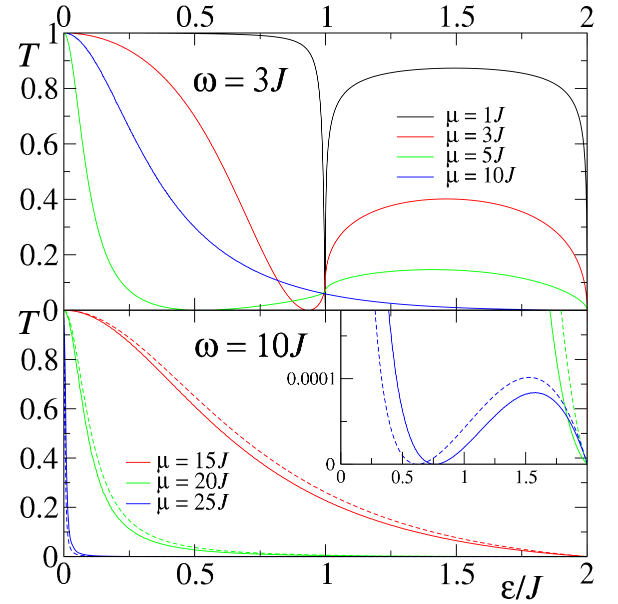

FIG. 3. Transmission coefficient as a function of incoming particle energy ϵ at $\omega = 3J$ (top) and $\omega = 10J$ (bottom). The dashed lines in the bottom plot depict the high-frequency approximation in Eq. (13). The inset shows an enlarged region of the resonance for $\mu = 25J$.

Since then BIC's have received extensive attention in the context of transport phenomena [29,39,40]. The suppression of transmission is closely related to the Fano effect in this case [41,42].

In order to illustrate the connection with the Fano effect the behavior as a function of incoming energy at fixed frequency $\omega = 3J$ is shown in Fig. 3 (top). The characteristic asymmetric line shape of Fano resonances is clearly visible. In analogy to the critical frequency in Eq. (7), it is possible to define a critical energy $\epsilon_c = \omega - 2J$, above which the first side chain supports an unbound solution. We observe that a sharp resonance occurs just below this energy for small μ which then broadens and moves quickly away from this point with increasing μ. The lower part of Fig. 3 shows the behavior for larger frequency $\omega = 10J$, where the resonances are further apart and less pronounced (see inset). In this limit the agreement with the high-frequency approximation in Eq. (13) fits reasonably well (dashed lines in Fig. 3). The drop of the transmission $T \to 0$ for $\epsilon \to 2J$ occurs due to the vanishing of the particle velocity $u_k \to 0$ and is not connected to any resonance phenomenon.

As shown in Fig. 3 for fixed μ and ω there is at most one energy with $T = 0$ and in some cases it is not possible to find a resonance at all, e.g., for $\omega = 3J$ and $\mu = 10J$. This is in contrast to the situation of a given energy discussed above in Fig. 2 where there are always one or more resonance frequencies for any value of μ.

In order to predict the location of the resonances with $T = 0$ we now follow the strategy to consider the eigenenergies of the decoupled side system in Fig. 1 using Eq. (5) with $\phi_{0,0} = 0$. In fact, the two sides for $n > 0$ and $n < 0$ have identical eigenenergies ϵ, due to the symmetry transformation $\phi_{j,n} \to (-1)^{n+j}\phi_{j,-n}$. Of course there are infinitely many eigenenergies, but only those inside the band $|\epsilon| < 2J$ are of interest. Let us focus on the resonances $T = 0$ close to the critical frequency $\omega \approx \omega_c$ in the limit of small $\mu \ll J$. In this case, Eq. (9) must still hold for $C_0 = 0$, with $\gamma_{n\neq 1} \gg 1$ and $\gamma_1 \ll 1$. Looking at the first few terms of the recurrence relation it becomes clear that the coefficients grow beyond bounds unless $1 - \gamma_1\gamma_2 \ll \gamma_1 \ll 1$. Solving for the frequency at which $\gamma_1\gamma_2 = 1$ we find for the resonance positions

$$\omega \approx \omega_c + \frac{\mu^4}{64J\big([4J-\epsilon]^2 - 4J^2\big)}, \qquad (14)$$

which is marked by dashed lines (red) in Fig. 2 and agrees well with the exact results. Using the condition $\gamma_1\gamma_2 = 1$, resonances can also be found at fixed ω for small deviations from the critical energy ϵ_c, which are again proportional to μ^4.

Conclusions. In summary we have developed a framework to study the transmission across an AC driven barrier connected to leads of finite bandwidth based on the Floquet formalism. The resulting transmission coefficient T can be calculated exactly and shows versatile tunability with frequency ω, energy ϵ, and impurity strength μ. At high frequencies $\omega \gg J$ the transmission can be expressed in terms of Bessel functions, which also appear in the description of so-called coherent destruction of tunneling. In this limit the oscillations can be averaged to form an effective quasistatic hopping $J_{\text{eff}} = J\mathcal{J}_0(\mu/\omega)$ [4,43]. In our case, a slightly more refined picture emerges in terms of Bessel functions with a fractional index $\nu = |n| \pm \epsilon/\omega$.

However, much more interesting effects appear at lower frequencies $\omega \approx \omega_c = 2J + |\epsilon|$ where there are sharp changes in T and a complete breakdown of the transmission $T = 0$ may appear even for arbitrarily small barriers μ. The explanation of such a *quantum resonance catastrophe* can be found in the dynamically created side-coupled chains in Fig. 1, which contain bound states for all energies *outside* the band for $\omega > \omega_c$. The effect of the local coupling μ between the chains is to push one energy from just above the band into the continuum. Thus effectively a discrete bound state in the continuum is formed, which is known to have drastic effects on the transmission [38] based on the Fano effect [41]. In fact, static side-coupled systems can also be used to engineer Fano resonances [42], but the virtual side-coupled systems in Fig. 1 by periodic driving are simpler and more versatile. The location of the resulting resonances for $\mu \to 0$ are predicted accurately by Eq. (14). The width of the resonance also changes dramatically near ω_c (proportionally to μ^{-4}). Therefore noise will become the limiting factor for observing a very sharp quantum resonance catastrophe. For example, in order to observe a suppression of transmission by a factor of ten for a small potential $\mu = 0.1J$, the uncertainty of the energy must be below $10^{-6}J$. On the other hand, there has been tremendous progress in stabilizing lasers and oscillators using a frequency comb, leading in some cases to world-record accuracy of up to 10^{-18} [44]. It is therefore promising to use the quantum resonance catastrophe in the design of an energy filter that limits the transmission at exactly one energy and in turn prepares reflected particles at a well-defined momentum (corresponding to a reflection grating in frequency). In this way the remarkable accuracy of oscillators and state-of-the-art lasers can be transferred to high-fidelity quantum state preparation as a tool in quantum technology. The sharp resonance catastrophe also presents a unique opportunity for the design of switches, where a huge change of transmission for small parameter changes is a desirable feature.

Acknowledgments. We thank Luis Foa, Pedro Orellana, Axel Pelster, and Luis Rosales for fruitful discussions. This research was financially supported by FONDECYT Grant No. 11110537, CONICYT Grant No. 63140250, and the German Research Foundation (DFG) via the SFB/TR49.

[1] Driven Quantum Systems, edited by W. Domcke, P. Hänggi, and D. Tannor, Chem. Phys. **217**, 117 (1997).

[2] M. Grifoni and P. Hänggi, Driven quantum tunneling, Phys. Rep. **304**, 229 (1998).

[3] For a review, see W. G. van der Wiel, S. De Franceschi, J. M. Elzerman, T. Fujisawa, S. Tarucha, and L. P. Kouwenhoven, Electron transport through double quantum dots, Rev. Mod. Phys. **75**, 1 (2002).

[4] G. Della Valle, M. Ornigotti, E. Cianci, V. Foglietti, P. Laporta, and S. Longhi, Visualization of Coherent Destruction of Tunneling in an Optical Double Well System, Phys. Rev. Lett. **98**, 263601 (2007).

[5] W. Li and L. E. Reichl, Floquet scattering through a time-periodic potential, Phys. Rev. B **60**, 15732 (1999).

[6] M. V. Entin and M. M. Mahmoodian, High-frequency blockade in tight-binding one-dimensional lattice with single vibrating site, Europhys. Lett. **84**, 47008 (2008)

[7] K. J. Savage, M. M. Hawkeye, R. Esteban, A. G. Borisov, J. Aizpurua, and J. J. Baumberg, Revealing the quantum regime in tunnelling plasmonics, Nature (London) **491**, 574 (2012).

[8] E. Kierig, U. Schnorrberger, A. Schietinger, J. Tomkovic, and M. K. Oberthaler, Single-Particle Tunneling in Strongly Driven Double-Well Potentials, Phys. Rev. Lett. **100**, 190405 (2008).

[9] A. Zenesini, H. Lignier, D. Ciampini, O. Morsch, and E. Arimondo, Coherent Control of Dressed Matter Waves, Phys. Rev. Lett. **102**, 100403 (2009).

[10] H. Miyake, G. A. Siviloglou, C. J. Kennedy, W. C. Burton, and W. Ketterle, Realizing the Harper Hamiltonian with Laser-Assisted Tunneling in Optical Lattices, Phys. Rev. Lett. **111**, 185302 (2013).

[11] S. E. Pollack, D. Dries, R. G. Hulet, K. M. F. Magalhaes, E. A. L. Henn, E. R. F. Ramos, M. A. Caracanhas, and V. S. Bagnato, Collective excitation of a Bose-Einstein condensate by modulation of the atomic scattering length, Phys. Rev. A **81**, 053627 (2010).

[12] M. Aidelsburger, M. Lohse, C. Schweizer, M. Atala, J. T. Barreiro, S. Nascimbne, N. R. Cooper, I. Bloch, and N. Goldman, Measuring the Chern number of Hofstadter bands with ultracold bosonic atoms, Nat. Phys. **11**, 162 (2015).

[13] V. Balzani, M. Venturi, and A. Credi, *Molecular Devices and Machines: A Journey into the Nanoworld* (John Wiley & Sons, New York, 2006).
[14] A. Nitzan and M. A. Ratner, Electron transport in molecular wire junctions, Science **300**, 1384 (2003).
[15] M. A. Reed, C. Zhou, C. Muller, T. Burgin, and J. Tour, Conductance of a molecular junction, Science **278**, 252 (1997).
[16] X. Cui, A. Primak, X. Zarate, J. Tomfohr, O. Sankey, A. Moore, T. Moore, D. Gust, G. Harris, and S. Lindsay, Reproducible measurement of single-molecule conductivity, Science **294**, 571 (2001).
[17] A. Aviram and M. A. Ratner, Molecular rectifiers, Chem. Phys. Lett. **29**, 277 (1974).
[18] K. Goser, P. Glösekötter, and J. Dienstuhl, *Nanoelectronics and Nanosystems: From Transistors to Molecular and Quantum Devices* (Springer Science & Business Media, Berlin, Heidelberg, 2004).
[19] G. Fagas, G. Cuniberti, and K. Richter, Electron transport in nanotube–molecular-wire hybrids, Phys. Rev. B **63**, 045416 (2001).
[20] G. Cuniberti, G. Fagas, and K. Richter, Fingerprints of mesoscopic leads in the conductance of a molecular wire, Chem. Phys. **281**, 465 (2002).
[21] L. Shen, M. Zeng, S.-W. Yang, C. Zhang, X. Wang, and Y. Feng, Electron transport properties of atomic carbon nanowires between graphene electrodes, J. Am. Chem. Soc. **132**, 11481 (2010).
[22] R. Gutiérrez, G. Fagas, G. Cuniberti, F. Grossmann, R. Schmidt, and K. Richter, Theory of an all-carbon molecular switch, Phys. Rev. B **65**, 113410 (2002).
[23] M. C. Rechtsman, J. M. Zeuner, Y. Plotnik, Y. Lumer, D. Podolsky, F. Dreisow, S. Nolte, M. Segev, and A. Szameit, Photonic Floquet topological insulators, Nature (London) **496**, 196 (2013).
[24] M. Bayindir, B. Temelkuran, and E. Ozbay, Tight-Binding Description of the Coupled Defect Modes in Three-Dimensional Photonic Crystals, Phys. Rev. Lett. **84**, 2140 (2000).
[25] Y. Plotnik, M. C. Rechtsman, D. Song, M. Heinrich, J. M. Zeuner, S. Nolte, Y. Lumer, N. Malkova, J. Xu, A. Szameit, Z. Chen, and M. Segev, Observation of unconventional edge states in photonic graphene, Nat. Mater. **13**, 57 (2014).
[26] I. Bloch, Ultracold quantum gases in optical lattices, Nat. Phys. **1**, 23 (2005).
[27] A. Vogler, R. Labouvie, G. Barontini, S. Eggert, V. Guarrera, and H. Ott, Dimensional Phase Transition from An Array of 1D Luttinger Liquids to a 3D Bose-Einstein Condensate, Phys. Rev. Lett. **113**, 215301 (2014).
[28] N. Spethmann, F. Kindermann, S. John, C. Weber, D. Meschede, and A. Widera, Dynamics of Single Neutral Impurity Atoms Immersed in an Ultracold Gas, Phys. Rev. Lett. **109**, 235301 (2012).
[29] See, for example: S. Longhi and G. Della Valle, Floquet bound states in the continuum, Sci. Rep. **3**, 2219 (2013).
[30] D. W. Hone and M. Holthaus, Locally disordered lattices in strong ac electric fields, Phys. Rev. B **48**, 15123 (1993).
[31] For a review, see B. Kaestner and V. Kashcheyevs, Non-adiabatic quantized charge pumping with tunable-barrier quantum dots: A review of current progress, Rep. Prog. Phys. **78**, 103901 (2015).
[32] C. Tomaras and S. Kehrein, Scaling approach for the time-dependent Kondo model, Europhys. Lett. **93**, 47011 (2011)
[33] A.-P. Jauho, N. S. Wingreen, and Y. Meir, Time-dependent transport in interacting and noninteracting resonant-tunneling systems, Phys. Rev. B **50**, 5528 (1994).
[34] G. Floquet, Sur les équations différentielles lináires à coefficients périodiques, Ann. de l'Ecole Norm. Sup. **12**, 47 (1883).
[35] O. Klein, Die Reflexion von Elektronen an einem Potentialsprung nach der relativistischen Dynamik von Dirac, Z. Phys. **53**, 157 (1929).
[36] Since there is no energy conservation, the particle may be transmitted or reflected into any of the unbound Floquet modes with $n \neq 0$.
[37] I. S. Gradshteyn and I. M. Ryzhik, *Table of Integrals, Series, and Products*, 5th edition (Academic Press, San Diego, CA, 1994).
[38] J. von Neumann and E. P. Wigner, Über merkwürdige diskrete Eigenwerte, Phys. Z. **30**, 465 (1929).
[39] F. H. Stillinger and D. R. Herrick, Bound states in the continuum, Phys. Rev. A **11**, 446 (1975).
[40] C. González-Santander, P. Orellana, and F. Dominguez-Adame, Bound states in the continuum driven by ac fields, Europhys. Lett. **102**, 17012 (2013).
[41] H. Friedrich and D. Wintgen, Interfering resonances and bound states in the continuum, Phys. Rev. A **32**, 3231 (1985); M. L. L. de Guevara, and P. A. Orellana, Electronic transport through a parallel-coupled triple quantum dot molecule: Fano resonances and bound states in the continuum, Phys. Rev. B **73**, 205303 (2006).
[42] A. E. Miroshnichenko and Y. S. Kivshar, Engineering Fano resonances in discrete arrays, Phys. Rev. E **72**, 056611 (2005).
[43] A. Rapp, X. Deng, and L. Santos, Ultracold Lattice Gases with Periodically Modulated Interactions, Phys. Rev. Lett. **109**, 203005 (2012); T. Wang, X.-F. Zhang, F. E. A. dos Santos, S. Eggert, and A. Pelster, Tuning the quantum phase transition of bosons in optical lattices via periodic modulation of the s-wave scattering length, Phys. Rev. A **90**, 013633 (2014).
[44] T. L. Nicholson *et al.*, Systematic evaluation of an atomic clock at 2×10^{-18} total uncertainty, Nat. Commun. **6**, 6896 (2015).